




Cite this: *RSC Adv.*, 2024, 14, 37196

The radical scavenging activity of 1-methyl-1,4-dihydronicotinamide: theoretical insights into the mechanism, kinetics and solvent effects†

Quan V. Vo, ^a Nguyen Thi Hoa^a and Adam Mechler ^{*b}

1,4-Dihydronicotinamide derivatives, including 1-methyl-1,4-dihydronicotinamide (MNAH), are derivatives of the active center of nicotinamide coenzyme (NADH) and are therefore potent radical scavengers. MNAH serves as a useful model of NADH that allows for modeling studies to address the activity of this important biomolecule. In this work, MNAH activity was evaluated against typical free radicals using quantum chemical calculations in physiological environments, with a secondary aim of comparing activity against two physiologically relevant radicals of markedly different stability, HO[•], and HOO[•], to establish which of these is a better model for assessing antioxidant capacity in physiological environments. The HO[•] + MNAH reaction exhibited diffusion-limited overall rate constants in all media, including the gas phase. The HOO[•] antiradical activity of MNAH was also good, with overall rate constants of 2.00×10^4 and $2.44 \times 10^6 \text{ M}^{-1} \text{ s}^{-1}$, in lipid and aqueous media, respectively. The calculated rate constant in water ($k_{\text{overall}}(\text{MNAH} + \text{HOO}^{\bullet}) = 3.84 \times 10^5 \text{ M}^{-1} \text{ s}^{-1}$, pH = 5.6) is in good agreement with the experimental data ($k_{\text{exp}}(\text{NADH} + \text{HOO}^{\bullet}) = (1.8 \pm 0.2) \times 10^5 \text{ M}^{-1} \text{ s}^{-1}$). In terms of mechanism, the H-abstraction of the C4–H bond characterized the HOO[•] radical scavenging activity of MNAH, whereas HO[•] could react with MNAH at several sites and following either of SET (in polar media), RAF, and FHT reactions, which could be ascribed to the high reactivity of HO[•]. For this reason the results suggest that activity against HOO[•] is a better basis for comparison of anti-radical potential. In the broader context, the HOO[•] scavenging activity of MNAH is better than that of reference antioxidants such as *trans*-resveratrol and ascorbic acid in the nonpolar environment, and Trolox in the aqueous physiological environment. Therefore, in the physiological environment, MNAH functions as a highly effective radical scavenger.

Received 6th October 2024
Accepted 14th November 2024

DOI: 10.1039/d4ra07184k

rsc.li/rsc-advances

1. Introduction

Reactive oxygen species (ROS) are molecules that are extremely reactive and are primarily produced by the mitochondrial electron transport chain.¹ Under normal circumstances, ROS are generated as natural biproducts of normal metabolic processes and also serve a variety of functions in healthy physiological processes. For example, they activate signaling pathways to initiate biological processes as “secondary messengers”.² Oxidative stress is the result of an imbalance between the antioxidant defense system and ROS production.³ It is also crucial to preserve the equilibrium of ROS in bone homeostasis and pathology.⁴ Nicotinamide coenzyme (NADH) is a natural redox factor that is crucial for the reduction of ROS; it is a ubiquitous hydride and electron source that participates

in a diverse array of biochemical processes that occur *in vivo*.^{5–7} The mechanism of oxidoreductase primarily relies on the cycling of nicotinamide adenine dinucleotide (NAD) and its reduced form, NADH. The NAD redox pair (NAD⁺/NADH) serves as a coenzyme essential for oxidoreductase metabolism.^{8–12}

Since the active center of NADH is dihydronicotinamide (Fig. 1), which contains two weak C4–H bonds; the radical scavenging could occur directly there following the formal hydrogen transfer mechanism.¹³ The nicotinamide component may also react with highly-reactive ROS, such as HO[•] radicals, through the radical adduct formation (RAF) and either the hydrogen transfer pathway or single electron transfer (SET). Nevertheless, this matter has not yet been thoroughly investigated.

The hydroxyl radical is a prevalent and highly reactive species among free radicals. It is identified as the primary effector of tissue damage caused by ionizing radiation and oxidative damage to DNA.^{14,15} Because of its high reactivity its physiological lifetime is short, therefore the ideal way of reducing oxidative stress due to HO[•] would be to inhibit the production of hydroxyl radicals.¹⁶ Due to its dominant role in pathologic processes it is quite common in the literature to

^aThe University of Danang – University of Technology and Education, Danang 550000, Vietnam. E-mail: vvquan@ute.udn.vn

^bDepartment of Biochemistry and Chemistry, La Trobe University, Victoria 3086, Australia. E-mail: a.mechler@latrobe.edu.au

† Electronic supplementary information (ESI) available. See DOI: <https://doi.org/10.1039/d4ra07184k>

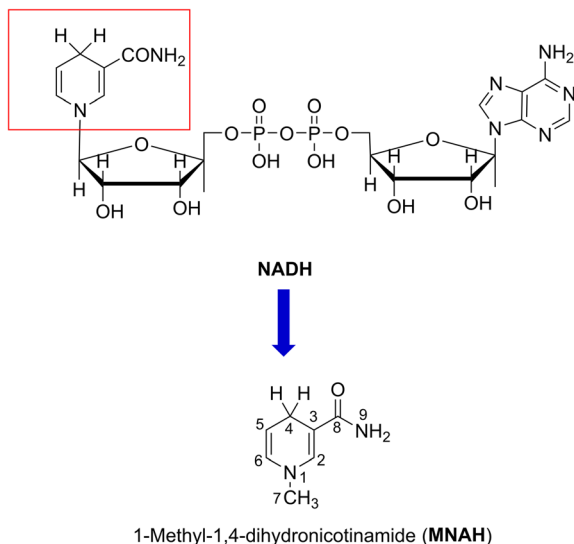



Fig. 1 The structure of MNAH.

investigate radical scavenging activity against the hydroxyl radical, and it is indeed crucial if the focus is on evaluating the degradation of organic compounds.^{17–19} On the other hand, the HO• model may not be an effective way to compare the radical scavenging activity of organic compounds due to the inherent high reactivity of this radical. A more representative model of the typical less reactive radicals is the HOO• radical, and thus it is a better alternative for computational studies to evaluate the yet unknown free radical scavenging activity of compounds.^{16,17,19} To highlight this issue in this study we examine and compare activity against HO• and HOO•.

Previous studies demonstrated that the HO•/HOO• radical scavenging activity of organic compounds can be accurately modeled by quantum chemical methods.^{20–22} Using this method, we modeled the kinetics and mechanism of the HO•/HOO• scavenging activity of 1-methyl-1,4-dihydronicotinamide (**MNAH**) (Fig. 1), the active center of **NADH**, in physiological environments.

2. Computational methods

The kinetic calculations in this study were conducted in accordance with the quantum mechanics-based test for overall free radical scavenging activity (QM-ORSA) protocol, combined with the SMD solvation model²³ procedure for pentyl ethanoate and water solvents.^{17,24–27} The traditional transition state theory (TST) at a temperature of 298.15 K and a standard state of 1 M was used to compute the rate constant (*k*) as outlined in eqn (1) by using the Eyringpy code.²⁶ (more information method in Table S1, ESI†):^{28–33}

$$k = \sigma \kappa \frac{k_B T}{h} e^{-(\Delta G^\ddagger)/RT} \quad (1)$$

where σ is the reaction symmetry number,^{34,35} κ stands for tunneling corrections that were calculated using Eckart barrier,³⁶ k_B is the Boltzmann constant, h is the Planck constant, ΔG^\ddagger is Gibbs free energy of activation.

Gaussian 16 software³⁷ was employed to conduct all calculations at the M06-2X/6-311++G(d,p) level of theory, which was previously identified as an appropriate model chemistry for this application.^{38,39}

3. Results and discussions

3.1. The radical scavenging in the gas phase

3.1.1. Thermodynamic study. Under conditions of non-polar media such as in the gas phase, the antiradical activity can follow either of three primary mechanisms: sequential electron transfer proton transfer (SETPT),^{40,41} formal hydrogen transfer (FHT),²⁵ or radical adduct formation (RAF) in the case of molecules with double bonds.⁴² To identify the most effective antioxidant mechanisms, we calculated the Gibbs free energy changes (ΔG°) in the gas phase for each reaction of **MNAH** with HOO• and HO• radicals in one of the following reactions: FHT, RAF, or single electron transfer (SET) for the SETPT reaction. The results are shown in Table 1.

The findings revealed that most reactions between HO• and **MNAH** were thermodynamically favorable ($\Delta G^\circ < 0$), except for the SET reaction ($\Delta G^\circ = 139.6 \text{ kcal mol}^{-1}$). The **MNAH** + HOO• reaction was only spontaneous at the FHT (C4–H, $\Delta G^\circ = -14.6 \text{ kcal mol}^{-1}$), whereas those of other mechanisms, such as the SET and FHT (C7–H and N9–H), are not thermodynamically spontaneous ($\Delta G^\circ = 5.1\text{--}144.3 \text{ kcal mol}^{-1}$). The H-abstraction of C4–H is the most preferred thermodynamically **MNAH** + HO• reaction ($\Delta G^\circ = -45.8 \text{ kcal mol}^{-1}$, BDE = $71.2 \text{ kcal mol}^{-1}$). Thus, this could make a significant contribution to the HO• radical scavenging activity of **MNAH**. Nevertheless, the **MNAH** + HO• reaction could also follow the RAF reactions at C2, C3, C5, and C6 and the FHT (C7–H) due to the low negative ΔG° values ($\Delta G^\circ = -17.4$ to $-26.1 \text{ kcal mol}^{-1}$). The HO•/HOO• radical scavenging activity of **MNAH** may not involve the H-abstraction of N9–H due to the high BDE and ΔG° values (BDE = $109.9 \text{ kcal mol}^{-1}$; $\Delta G^\circ = -6.2$ and $25.1 \text{ kcal mol}^{-1}$ for HO• and HOO• radicals, respectively). Consequently, the kinetics of the HO•/HOO• radicals scavenging activity of **MNAH** were evaluated at all of the sites of spontaneous reactions ($\Delta G^\circ < 0$).

3.1.2. Kinetic study. In the initial kinetic evaluation, the potential energy surfaces (PES) were first computed; the findings are presented in Fig. 2. The highest reaction barrier

Table 1 The computed BDE and ΔG° (in kcal mol^{-1}) following the RAF, FHT, and SET mechanisms of the **MNAH** + HO•/HOO• reactions

Mechanisms	Positions	BDE	ΔG°	
			HO•	HOO•
FHT	C4–H	71.2	−45.8	−14.6
	C7–H	90.9	−26.1	5.1
	N9–H	109.9	−6.2	25.1
RAF	C2		−23.1	
	C3		−17.4	
	C5		−25.7	
	C6		−20.2	
SET			139.6	144.3



(12.5 kcal mol⁻¹) for the **MNAH** + HO[•] reaction is observed at the FHT of the N9–H bond, while the C4 position of **MNAH** presented the lowest reaction barrier value (0.1 kcal mol⁻¹). The RAF at C2, C3, and C5 positions had reaction barriers of 2.7, 2.0, and 3.5 kcal mol⁻¹, respectively, whereas those of C6 and C7–H were 4.6 and 8.3 kcal mol⁻¹, respectively. Based on these results, the dominant **MNAH** + HO[•] reactions are the addition of the HO[•] radical at the C2, C3, or C5 positions and the FHT reaction of the C4–H bonds, while the H-abstraction of **MNAH** by HO[•] radicals *via* the C7–H and N9–H bonds would not contribute to the activity. The HOO[•] radical scavenging reaction is defined by the H-abstraction at the C4–H bond with the low reaction barrier at 0.1 kcal mol⁻¹.

The kinetics of the **MNAH** + HO[•]/HOO[•] reactions were calculated by using the QM-ORSA methodology.¹⁷ The results are presented in Table 2, whereas the optimized structures and the SOMO orbitals of transition states (TS) are shown in Fig. 3 and S1, ESI,† respectively. In the gas phase, the FHT reaction of the C4–H with HO[•] radicals was barrierless ($\Delta G^\ddagger \approx 0$ kcal mol⁻¹, $k_{\text{Eck}} = 6.02 \times 10^{12}$ M⁻¹ s⁻¹, $\Gamma = 27.1\%$), whereas that of C7–H and N9–H bonds had no contribution to the radical scavenging activity with $k_{\text{Eck}} = 1.39 \times 10^{10}$ M⁻¹ s⁻¹ ($\Gamma = 0.1\%$) and 5.60×10^7 M⁻¹ s⁻¹ ($\Gamma = 0.0\%$), respectively. At the same time, the RAF reactions at C2, C3, and C5 form a substantial part of the overall **MNAH** + HO[•] reaction with $\Delta G^\ddagger \approx 0$ kcal mol⁻¹, $k_{\text{Eck}} = 6.02 \times 10^{12}$ M⁻¹ s⁻¹, $\Gamma = 27.1\%$ for each position. The addition reaction at the C6 location contributed only about 1.1% to the overall rate constant. Thus in the gas phase, the **MNAH** + HO[•] reaction was rapid and defined by the FHT(C4–H) and RAF(C2, C3, and C5) mechanisms with the overall rate constant $k_{\text{overall}} = 2.22 \times 10^{13}$ M⁻¹ s⁻¹, whereas the **MNAH** + HOO[•] reaction was moderate and characterized by the

Table 2 Computed ΔG^\ddagger (in kcal mol⁻¹), κ , k_{Eck} (M⁻¹ s⁻¹) and branching ratios ($\Gamma\%$) for the **MNAH** + HO[•]/HOO[•] reactions^a

Radicals	Mechanisms	Positions	ΔG^{\ddagger}	κ	k_{Eck}	Γ
HO \cdot	FHT	C4-H	0.0	1.0	6.02×10^{12}	27.1
		C7-H	3.9	1.6	1.39×10^{10}	0.1
		N9-H	8.9	30.2	5.60×10^7	0.0
	RAF	C2	0.0	1.0	6.02×10^{12}	27.1
		C3	0.0	1.0	6.02×10^{12}	27.1
		C5	0.3	1.0	3.91×10^{12}	17.6
		C6	2.0	1.0	2.35×10^{11}	1.1
k_{overall}					2.22×10^{13}	
HOO \cdot	FHT	C4-H	9.1	2.1	2.83×10^6	100.0
$^a \Gamma = k_{\text{Eck}} \cdot 100 / k_{\text{overall}}$.						

^a $\Gamma = k_{\text{Eck}} \cdot 100 / k_{\text{overall}}$.

FHT(C4–H) with $k_{\text{overall}} = 2.83 \times 10^6$ M⁻¹ s⁻¹. The main products of the **MNAH** + HO[•] reaction in the gas phase were **P-C2** (27.1%), **P-C3** (27.1%), **P-C4** (27.1%), and **P-C5** (17.6%), whereas for the **MNAH** + HOO[•] reaction **P-C4**(HOO) was the only product (100%) (Fig. 2 and Table 2).

The extremely high theoretical rate constant for the **MNAH** + HO[•] reaction ($k_{\text{overall}} = 2.22 \times 10^{13}$ M⁻¹ s⁻¹) suggests that the reaction is diffusion-limited even in the gas phase where the collision rate at the given temperature would limit the reaction to 10^9 – 10^{10} M⁻¹ s⁻¹. Hence the activity against HO[•] radical is not a useful basis for comparison. On the other hand, the HOO[•] radical scavenging activity of **MNAH** is comparable to the reference antioxidant Trolox ($k_{(\text{HOO}^\bullet + \text{Trolox})} = 1.87 \times 10^7$ M⁻¹ s⁻¹).³³ This suggests that **MNAH** may exhibit a good radical scavenging activity in the physiological environment that warrants further investigation.

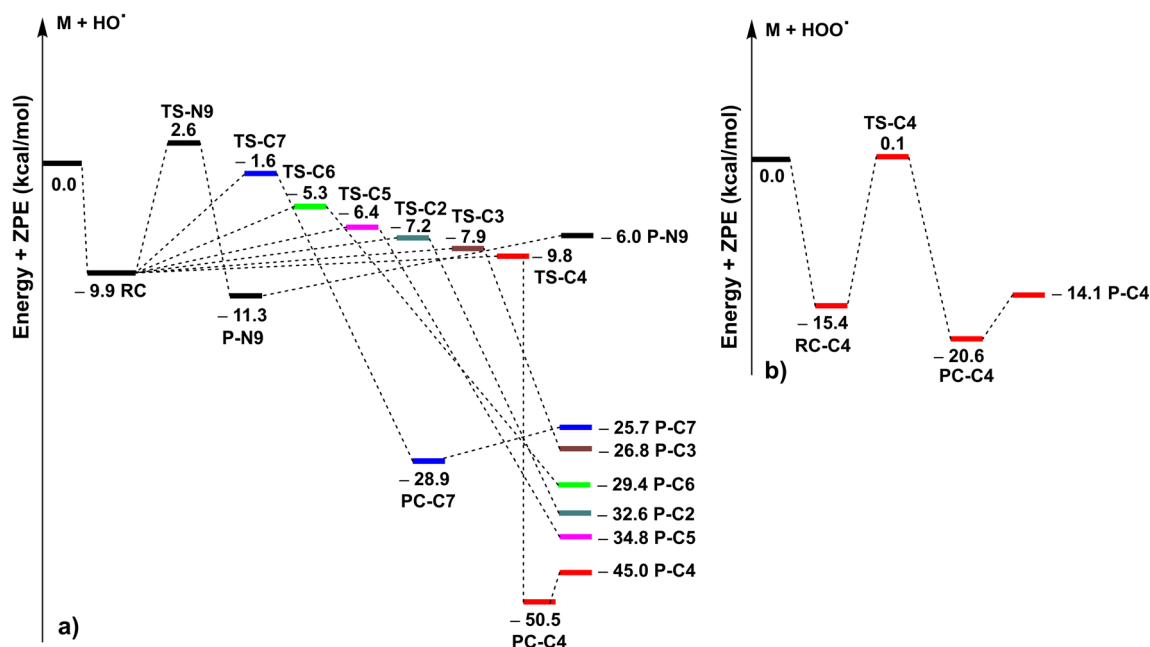


Fig. 2 The PES of the **MNAH** + HO[•] (a)/HOO[•] (b) reactions at the spontaneous reactions (RC: pre-complex; TS: transition state; PC: post-complex; P: product).



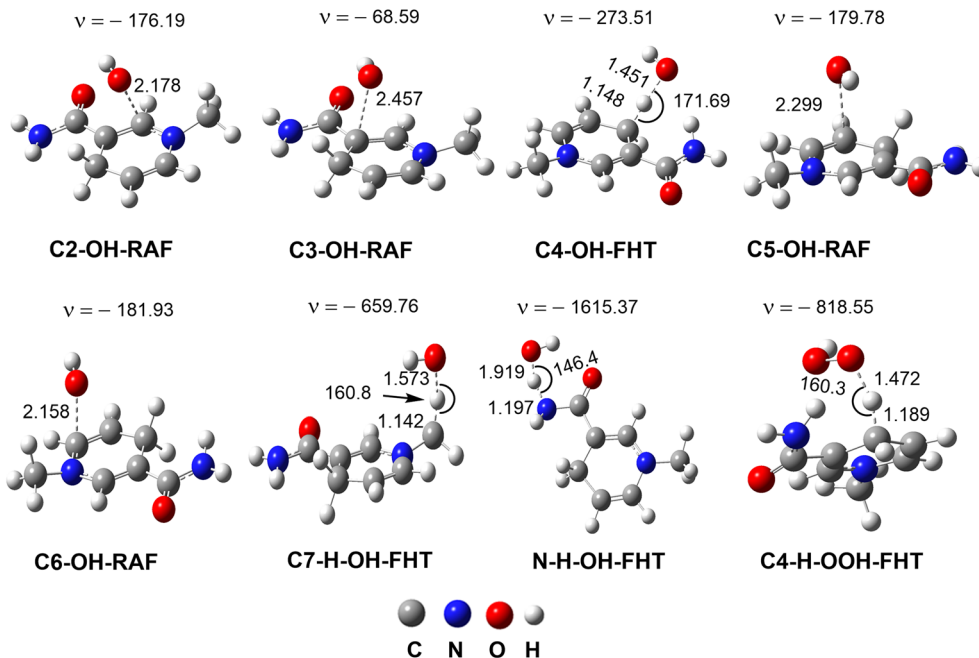


Fig. 3 The optimized transition states of the RAF and FHT mechanisms in the **MNAH** + $\text{HO}^\bullet/\text{HOO}^\bullet$ reactions (ν in cm^{-1} , bond length in Å).

3.2. The $\text{HO}^\bullet/\text{HOO}^\bullet$ scavenging activity of **MNAH** in the physiological environments

3.2.1. Acid-base equilibrium of **MNAH in water.** Sequential proton loss electron transfer (SPLET) is the principal antioxidant mechanism that controls the radical scavenging efficacy of nitrogenous substances in aqueous solutions.⁴³ This is mainly attributable to the spontaneous deprotonation, which removes the potential barrier of the initial phase. Therefore, this section evaluated the deprotonation equilibria of **MNAH**. The pK_a value was determined using a literature method,⁴⁴ as illustrated in Fig. 4. It was determined that the pK_a value of **MNAH** in an aqueous solution was -1.45 (N1-H). **MNAH** molecule is exclusively present in a neutral state (**MNAH**, 100%) in the physiological aqueous solution. Thus, the neutral state was assessed in the $\text{HO}^\bullet/\text{HOO}^\bullet$ scavenging activity of **MNAH** in the physiological environments (water and pentyl ethanoate).

3.2.2. Kinetic study. The $\text{HO}^\bullet/\text{HOO}^\bullet$ antiradical activity of **MNAH** in physiological media was calculated using the QM-ORSA protocol.^{17,19} The overall rate constants of the $\text{HO}^\bullet/\text{HOO}^\bullet$ + **MNAH** reaction were calculated using eqn (2)–(5). The findings are presented in Table 3.

In pentyl ethanoate:

$$k_{\text{overall}}(\text{HO}^\bullet) = \Sigma k_{\text{app}}(\text{RAF}) + \Sigma k_{\text{app}}(\text{FHT}) \quad (2)$$

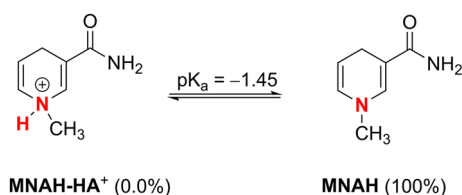


Fig. 4 Dissociation equilibria of **MNAH** at $\text{pH} = 7.4$.

$$k_{\text{overall}}(\text{HOO}^\bullet) = k_{\text{app}}(\text{FHT}(\text{C4-H})) \quad (3)$$

In water:

$$k_{\text{overall}}(\text{HO}^\bullet) = k_{\text{f}}(\text{SET}) + \Sigma k_{\text{f}}(\text{RAF}) + \Sigma k_{\text{f}}(\text{FHT}) \quad (4)$$

$$k_{\text{overall}}(\text{HOO}^\bullet) = k_{\text{f}}(\text{FHT}) + k_{\text{f}}(\text{SET}) \quad (5)$$

The k_{overall} values for the **MNAH** + HO^\bullet reaction in the nonpolar and aqueous environments were 1.69×10^{10} and $2.77 \times 10^{10} \text{ M}^{-1} \text{ s}^{-1}$, respectively. The k_{overall} of the **MNAH** + HOO^\bullet reaction is slower compared to the hydroxyl radical, with values of 2.00×10^4 and $2.44 \times 10^6 \text{ M}^{-1} \text{ s}^{-1}$ in the pentyl ethanoate and water solvents, respectively. It is important to notice that the pK_a value of the HOO^\bullet radical is 4.88. Consequently, the molar fraction of HOO^\bullet is 0.137 at $\text{pH} = 5.6$, resulting in a $k_{\text{overall}}(\text{MNAH} + \text{HOO}^\bullet)$ of $3.84 \times 10^5 \text{ M}^{-1} \text{ s}^{-1}$. This is in excellent agreement with the experimental data ($k_{\text{exp}}(\text{NADH} + \text{HOO}^\bullet) = (1.8 \pm 0.2) \times 10^5 \text{ M}^{-1} \text{ s}^{-1}$).⁴⁵ It was found that the HO^\bullet scavenging activity of **MNAH** was defined by the FHT of C4-H and C7-H positions (31.9%) and RAF (68.0%) reactions in the nonpolar environment. Conversely, the H-abstraction of N9-H bond did not contribute to the **MNAH** + HO^\bullet reaction. On the other hand, the H-abstraction of the C4-H bond dominated the activity against HOO^\bullet (100%).

The HO^\bullet antiradical activity in the polar environment is a combination of all analyzed mechanisms (FHT (32.9%), SET (26.7%) and RAF (40.4%)). Formal hydrogen transfer was the driving force behind the activity against the HOO^\bullet radical, where the SET reaction contributed only 1.8% of the overall rate constant. Based on the findings, the FHT and RAF reactions with HO^\bullet radicals in the aqueous physiological environment were barrierless ($\Delta G^\ddagger \approx 0 \text{ kcal mol}^{-1}$). Consequently, the k_{app} values of these processes were diffusion-limited (cannot exceed



Table 3 The computed ΔG^\ddagger (in kcal mol⁻¹), branching ratios ($\Gamma\%$), and k_{app} , k_f , k_{overall} , (M⁻¹ s⁻¹) of the reaction between **MNAH** and HO[•]/HOO[•] in the physiological environment

Radicals	Mechanism	Pentyl ethanoate					Water				
		ΔG^\ddagger	κ	k_{app}	Γ		ΔG^\ddagger	κ	k_{app}	k_f	Γ
HO [•]	SET						2.5	4.6 ^a	7.40×10^9	7.40×10^9	26.7
	FHT	C4-H	~0	1.0	3.20×10^9	18.9	~0	1.0	3.10×10^9	3.10×10^9	11.2
		C7-H	4.4	1.8	2.20×10^9	13.0	~0	1.0	3.10×10^9	3.10×10^9	11.2
		N9-H	12.0	37.6	3.80×10^5	0.0	~0	1.0	2.90×10^9	2.90×10^9	10.5
	RAF	C2	1.7	1.0	2.60×10^9	15.4	~0	1.0	2.60×10^9	2.60×10^9	9.4
		C3	1.5	1.0	3.20×10^9	18.9	~0	1.0	3.00×10^9	3.00×10^9	10.8
		C5	1.0	1.0	3.10×10^9	18.3	~0	1.0	3.00×10^9	3.00×10^9	10.8
		C6	2.0	1.0	2.60×10^9	15.4	~0	1.0	2.60×10^9	2.60×10^9	9.4
		k_{overall}			1.69×10^{10}					2.77×10^{10}	
	SET						11.1	16.6 ^a	4.30×10^4	4.30×10^4	1.8
HOO [•]	FHT	C4-H	11.9	1.6	2.00×10^4		9.3	2.4	2.40×10^6	2.40×10^6	98.2
	k_{overall}				2.00×10^4					2.44×10^6	

^a The nuclear reorganization energy (λ , in kcal mol⁻¹).

diffusion rates k_D) and accounted for approximately 73.3% of the overall rate constant.

According to the results the **MNAH** + HO[•] reaction is practically diffusion-limited under all conditions, including the gas phase. On the other hand, the activity against HOO[•] was more nuanced. **MNAH** exhibits a higher HOO[•] antiradical activity in the lipid medium than *trans*-resveratrol (~1.5 times, $k = 1.31 \times 10^4 \text{ M}^{-1} \text{ s}^{-1}$)⁴⁶ and ascorbic acid (~3.5 times, $k = 5.71 \times 10^3 \text{ M}^{-1} \text{ s}^{-1}$),¹⁷ but it is inferior to Trolox (~5.0 times, $k = 1.00 \times 10^5 \text{ M}^{-1} \text{ s}^{-1}$).³³ In the polar medium **MNAH** exhibits a higher activity than Trolox (~18.5 times, $k = 1.30 \times 10^5 \text{ M}^{-1} \text{ s}^{-1}$),³³ but it is weaker than ascorbic acid and *trans*-resveratrol. The markedly different activity against the two radicals is arguably the result of the high reactivity of HO[•] and not the exceptional specific activity of **MNAH** in targeting and eliminating HO[•]. Thus our results underscore the importance of comparing antioxidant activity against the less reactive free radicals that have longer lifetimes under physiological conditions. Nevertheless, our results suggest that **MNAH** is an efficient radical scavenger in key physiological environments.

4. Conclusions

The radical scavenging activity of **MNAH** against HO[•] and HOO[•] was assessed through density functional theory calculations. In the lipid and water media, the k_{overall} values of the HO[•] + **MNAH** reaction were 1.69×10^{10} and $2.77 \times 10^{10} \text{ M}^{-1} \text{ s}^{-1}$, respectively. The HOO[•] radical scavenging activity was measured at 2.00×10^4 and $2.44 \times 10^6 \text{ M}^{-1} \text{ s}^{-1}$. In water, at pH = 5.6, the calculated rate constant ($k_{\text{overall}}(\text{MNAH} + \text{HOO}^\bullet) = 3.84 \times 10^5 \text{ M}^{-1} \text{ s}^{-1}$) is in good agreement with the experimental data ($k_{\text{exp}}(\text{NADH} + \text{HOO}^\bullet) = (1.8 \pm 0.2) \times 10^5 \text{ M}^{-1} \text{ s}^{-1}$) and could verify the accuracy of the computing method. In both nonpolar and polar media, the HOO[•] antiradical activity of **MNAH** was defined by the H-abstraction of the C4-H bond, whereas the HO[•] antiradical activity was determined by a combination of the SET (in polar media), RAF, and FHT reactions. The hydroperoxyl radical

scavenging activity of **MNAH** is greater than that of *trans*-resveratrol and ascorbic acid in the lipid medium, and Trolox in the aqueous physiological environment. The results have verified the potent radical scavenger role of **MNAH** in physiological environments, also highlighting that HOO[•] is a better model for comparing antiradical activity than the highly reactive HO[•].

Data availability

The data supporting this article have been included as part of the ESI.†

Conflicts of interest

There are no conflicts to declare.

Acknowledgements

This research is funded by Funds for Science and Technology Development of the University of Danang under project number B2021-DN01-01 (Q. V. V.).

References

- 1 A. A. Alfadda and R. M. Sallam, *BioMed Res. Int.*, 2012, **2012**, 936486.
- 2 R. L. Auten and J. M. Davis, *Pediatr. Res.*, 2009, **66**, 121–127.
- 3 J. S. Kimball, J. P. Johnson and D. A. Carlson, *J. Bone Jt. Surg.*, 2021, **103**, 1451–1461.
- 4 R. S. Balaban, S. Nemoto and T. Finkel, *Cell*, 2005, **120**, 483–495.
- 5 S. Immanuel, R. Sivasubramanian, R. Gul and M. A. Dar, *Chem.-Asian J.*, 2020, **15**, 4256–4270.
- 6 S. Zhang, J. Shi, Y. Chen, Q. Huo, W. Li, Y. Wu, Y. Sun, Y. Zhang, X. Wang and Z. Jiang, *ACS Catal.*, 2020, **10**, 4967–4972.



- 7 T. Knaus, C. E. Paul, C. W. Levy, S. De Vries, F. G. Mutti, F. Hollmann and N. S. Scrutton, *J. Am. Chem. Soc.*, 2016, **138**, 1033–1039.
- 8 H. Wu, C. Tian, X. Song, C. Liu, D. Yang and Z. Jiang, *Green Chem.*, 2013, **15**, 1773–1789.
- 9 X. Wang, T. Saba, H. H. Yiu, R. F. Howe, J. A. Anderson and J. Shi, *Chem*, 2017, **2**, 621–654.
- 10 S.-J. Lin and L. Guarente, *Curr. Opin. Cell Biol.*, 2003, **15**, 241–246.
- 11 F. H. Ahmed, A. E. Mohamed, P. D. Carr, B. M. Lee, K. Condic-Jurkic, M. L. O'Mara and C. J. Jackson, *Protein Sci.*, 2016, **25**, 1692–1709.
- 12 T. Rawling, H. MacDermott-Opeskin, A. Roseblade, C. Pazderka, C. Clarke, K. Bourget, X. Wu, W. Lewis, B. Noble and P. A. Gale, *Chem. Sci.*, 2020, **11**, 12677–12685.
- 13 Y.-H. Fu, Z. Wang, K. Wang, G.-B. Shen and X.-Q. Zhu, *RSC Adv.*, 2022, **12**, 27389–27395.
- 14 L. P. Candeias and S. Steenken, *Chem.–Eur. J.*, 2000, **6**, 475–484.
- 15 C. Chatgililoglu, M. D'Angelantonio, M. Guerra, P. Kaloudis and Q. G. Mulazzani, *Angew. Chem., Int. Ed.*, 2009, **48**, 2214–2217.
- 16 A. Galano and J. Raúl Alvarez-Idaboy, *Int. J. Quantum Chem.*, 2019, **119**, e25665.
- 17 A. Galano and J. R. Alvarez-Idaboy, *J. Comput. Chem.*, 2013, **34**, 2430–2445.
- 18 T. Marino, A. Galano and N. Russo, *J. Phys. Chem. B*, 2014, **118**, 10380–10389.
- 19 Q. V. Vo, M. V. Bay, P. C. Nam, D. T. Quang, M. Flavel, N. T. Hoa and A. Mechler, *J. Org. Chem.*, 2020, **85**, 15514–15520.
- 20 H. Boulebd, N. M. Tam, A. Mechler and Q. V. Vo, *New J. Chem.*, 2020, **44**, 16577–16583.
- 21 F. Sarraimi, L.-J. Yu and A. Karton, *J. Comput.-Aided Mol. Des.*, 2017, **31**, 905–913.
- 22 A. Karton, R. J. O'Reilly, D. I. Pattison, M. J. Davies and L. Radom, *J. Am. Chem. Soc.*, 2012, **134**, 19240–19245.
- 23 M. Carreon-Gonzalez, A. Vivier-Bunge and J. R. Alvarez-Idaboy, *J. Comput. Chem.*, 2019, **40**, 2103–2110.
- 24 J. R. I. Alvarez-Idaboy and A. Galano, *J. Phys. Chem. B*, 2012, **116**, 9316–9325.
- 25 A. Galano and J. Raúl Alvarez-Idaboy, *Int. J. Quantum Chem.*, 2019, **119**, e25665.
- 26 E. Dzib, J. L. Cabellos, F. Ortíz-Chi, S. Pan, A. Galano and G. Merino, *Int. J. Quantum Chem.*, 2019, **119**, e25686.
- 27 E. Dzib, J. L. Cabellos, F. Ortiz-Chi, S. Pan, A. Galano and G. Merino, *Eyringpy 1.0.2*, Cinvestav, Mérida, Yucatán, 2018.
- 28 M. G. Evans and M. Polanyi, *Trans. Faraday Soc.*, 1935, **31**, 875–894.
- 29 H. Eyring, *J. Chem. Phys.*, 1935, **3**, 107–115.
- 30 D. G. Truhlar, W. L. Hase and J. T. Hynes, *J. Phys. Chem.*, 1983, **87**, 2664–2682.
- 31 T. Furuncuoglu, I. Ugur, I. Degirmenci and V. Aviyente, *Macromolecules*, 2010, **43**, 1823–1835.
- 32 E. Vélez, J. Quijano, R. Notario, E. Pabón, J. Murillo, J. Leal, E. Zapata and G. Alarcón, *J. Phys. Org. Chem.*, 2009, **22**, 971–977.
- 33 H. Boulebd, A. Mechler, N. T. Hoa and Q. Van Vo, *New J. Chem.*, 2020, **44**, 9863–9869.
- 34 E. Pollak and P. Pechukas, *J. Am. Chem. Soc.*, 1978, **100**, 2984–2991.
- 35 A. Fernández-Ramos, B. A. Ellingson, R. Meana-Pañeda, J. M. Marques and D. G. Truhlar, *Theor. Chem. Acc.*, 2007, **118**, 813–826.
- 36 C. Eckart, *Phys. Rev.*, 1930, **35**, 1303.
- 37 M. J. Frisch, G. W. Trucks, H. B. Schlegel, G. E. Scuseria, M. A. Robb, J. R. Cheeseman, G. Scalmani, V. Barone, B. Mennucci, G. A. Petersson, H. Nakatsuji, M. Caricato, X. Li, H. P. Hratchian, A. F. Izmaylov, J. Bloino, G. Zheng, J. L. Sonnenberg, M. Hada, M. Ehara, K. Toyota, R. Fukuda, J. Hasegawa, M. Ishida, T. Nakajima, Y. Honda, O. Kitao, H. Nakai, T. Vreven, J. A. Montgomery, J. E. Peralta, F. Ogliaro, M. Bearpark, J. J. Heyd, E. Brothers, K. N. Kudin, V. N. Staroverov, R. Kobayashi, J. Normand, K. Raghavachari, A. Rendell, J. C. Burant, S. S. Iyengar, J. Tomasi, M. Cossi, N. Rega, J. M. Millam, M. Klene, J. E. Knox, J. B. Cross, V. Bakken, C. Adamo, J. Aramillo, R. Gomperts, R. E. Stratmann, O. Yazyev, A. J. Austin, R. Cammi, C. Pomelli, J. W. Ochterski, R. L. Martin, K. Morokuma, V. G. Zakrzewski, G. A. Voth, P. Salvador, J. J. Dannenberg, S. Dapprich, A. D. Daniels, Ö. Farkas, J. B. Foresman, J. V. Ortiz, J. Cioslowski and D. J. Fox, *Gaussian 16*, Revision A.03, Gaussian, Inc., Wallingford CT, 2016.
- 38 A. Galano and J. R. Alvarez-Idaboy, *J. Comput. Chem.*, 2014, **35**, 2019–2026.
- 39 Y. Zhao and D. G. Truhlar, *J. Phys. Chem. A*, 2008, **112**, 1095–1099.
- 40 K. U. Ingold and D. A. Pratt, *Chem. Rev.*, 2014, **114**, 9022–9046.
- 41 A. Galano, G. Mazzone, R. Alvarez-Diduk, T. Marino, J. R. Alvarez-Idaboy and N. Russo, *Annu. Rev. Food Sci. Technol.*, 2016, **7**, 335–352.
- 42 C. Iuga, J. R. Alvarez-Idaboy and A. Vivier-Bunge, *J. Phys. Chem. B*, 2011, **115**, 12234–12246.
- 43 Q. V. Vo, N. T. Hoa, P. C. Nam, T. Q. Duong and A. Mechler, *New J. Chem.*, 2023, **47**, 10381–10390.
- 44 A. Galano, A. Pérez-González, R. Castañeda-Arriaga, L. Muñoz-Rugeles, G. Mendoza-Sarmiento, A. Romero-Silva, A. Ibarra-Escutia, A. M. Rebollar-Zepeda, J. R. León-Carmona, M. A. Hernández-Olivares and J. R. Alvarez-Idaboy, *J. Chem. Inf. Model.*, 2016, **56**, 1714–1724.
- 45 A. Nadezhdin and H. Dunford, *J. Phys. Chem.*, 1979, **83**, 1957–1961.
- 46 M. Cordova-Gomez, A. Galano and J. R. Alvarez-Idaboy, *RSC Adv.*, 2013, **3**, 20209–20218.

